

Efficient Rule Learning with Template Saturation for Knowledge Graph Completion

Yulong Gu, Yu Guan, Paolo Missier

School of Computing

Newcastle University, Newcastle upon Tyne, UK

{y.gu11, yu.guan, paolo.missier}@ncl.ac.uk

Abstract

The logic-based methods that learn first-order rules from knowledge graphs (KGs) for knowledge graph completion (KGC) task are desirable in that the learnt models are inductive, interpretable and transferable. The challenge in such rule learners is that the expressive rules are often buried in vast rule space, and the procedure of identifying expressive rules by measuring rule quality is costly to execute. Therefore, optimizations on rule generation and evaluation are in need. In this work, we propose a novel bottom-up probabilistic rule learner that features: 1.) a two-stage procedure for optimized rule generation where the system first generalizes paths sampled from a KG into template rules that contain no constants until a certain degree of template saturation is achieved and then specializes template rules into instantiated rules that contain constants; 2.) a grouping technique for optimized rule evaluation where structurally similar instantiated rules derived from the same template rules are put into the same groups and evaluated collectively over the groupings of the deriving template rules. Through extensive experiments over large benchmark datasets on KGC task, our algorithm demonstrates consistent and substantial performance improvements over all of the state-of-the-art baselines.

1 Introduction

Knowledge graph completion (KGC) has attracted many attentions in the last decade with the proliferation of large knowledge bases (KBs) such as NELL (Mitchell et al. 2018), Freebase (Bollacker et al. 2008) and YAGO (Hofstatter et al. 2013). Such KBs can be expressed by knowledge graphs (KGs) where nodes and directed edges represent entities and relations between entities, respectively. Since these large KGs are created by harvesting triples from semi-structured data sources on the web, they are inherently incomplete and error-prone. Methods for KGC aim to predict missing facts and verify the correctness of existing ones. There are many approaches that have been proposed in recent years to handle the KGC task, including the embedding methods (Cai, Zheng, and Chang 2018; Zhou et al. 2019) that embed items in KGs into continuous vector space for easy manipulation while preserving the inherent structure; the logic-based methods (Das et al. 2018; Meilicke et al. 2019; Sadeghian et al. 2019) that learn a set of first-order rules from KGs to infer missing facts and explain predictions; and hybrid systems that either use rules to

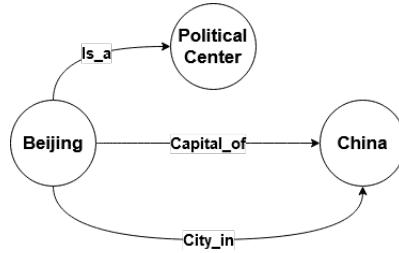


Figure 1: A small knowledge graph.

constrain embeddings (Guo et al. 2018; Niu et al. 2020), or learn embeddings to help refine rules (Pellissier et al. 2017; Ho et al. 2018). In comparison to embedding methods, logic-based ones are naturally interpretable, transferable and capable of inductive inference. Although many novel logic-based formulations have been proposed, in this work, we focus on developing classic inductive rule learners that explore discrete rule space using subsumption operators and score rules with statistical measures.

1.1 Problem

The balance between rule space complexity and system scalability is the main challenge of inductive rule learning. The complexity of a rule space is mainly decided by the choice of language bias that dictates what types of rules to include. Let us take the evolution of Path Ranking Algorithms (PRAs) as an example. PRA (Lao, Mitchell, and Cohen 2011) uses random walkers to extract a certain type of rules - the Closed Abstract Rules (CARs) which are sequences of predicates that connect entity pairs of learning targets in a KG. For instance in Figure.1, given predicate $Capital_of(X, Y)$ as the learning target and entity pair $(Beijing, China)$ as a positive instance, the rule:

$$f_0 = Capital_of(X, Y) \leftarrow City_in(X, Y)$$

is a CAR that translates as if a city X is in a country Y , then X is the capital of Y , which is wrong in most cases. To be able to describe targets in more detail, Cor-PRA (Lao, Minkov, and Cohen 2015) proposes to include Tail Anchored Rules (TARs), a type of rules with the last variable being substituted by a constant, for better expressivity.

Again in Figure.1, the conjunction of the TAR:

$$f_1 = \text{Capital_of}(X, Y) \leftarrow \text{Is_a}(X, \text{'Political Center'})$$

and the CAR f_0 is translated as if a city X is in a country Y , and X is a political center of Y , then X is the capital of Y . By including more types of rules, a rule space tends to become more complex and expressive, and is thus more likely to entail explosion in size, which often makes exploration of the rule space very expensive or simply infeasible. An ideal rule learner should be able to mine rules from complex rule space in reasonable runtime, and to achieve this, optimizations on procedures involved in the rule learning process are needed. There are two major procedures in the process of rule learning: the rule generation procedure and the rule evaluation procedure.

Rule Generation Procedure It decides how to explore a target rule space constrained by a given language bias and when to stop the exploration. A majority of existing works stop the exploration when entirely or a sampled subspace of the target rule space is explored. For instances, AMIE+ (Galárraga et al. 2015) searches the complete target rule space, and PRA (Lao, Mitchell, and Cohen 2011) and RuleN (Meilicke et al. 2018) search a sampled subspace by using random walkers and traversers starting from a subset of positive instances, respectively. As the exploration is not guided, it is often inefficient and hard to control. AnyBURL (Meilicke et al. 2019) proposes to control the progress of exploration using the saturation of rules. Specifically, rules of length n are mined in batches where rules mined in previous batches are considered as known rules, and if the proportion of known rules in current batch is above a saturation threshold, the system considers there is a saturation of rules of length n , and then either progresses to mine rules of length $n + 1$ or terminates. Although being more controllable than other methods, AnyBURL has trouble progressing to mine longer instantiated rules that contain constants on large KGs because the saturation is measured over all of the instantiated rules learnt for all learning targets, which makes it hard to converge.

Rule Evaluation procedure It decides what the rule quality measure is and how to plan the evaluation executions. Most of the existing works employ statistical measures such as confidence and support (Galárraga et al. 2015) to reflect rule quality. The statistical measures are costly to compute for a rule in that it requires the system to ground the rule using a backward tracking algorithm which is exponentially complex. However, a majority of existing works evaluate every mined rule individually, which leads to the main scalability bottleneck. Recent works propose to incorporate pre-trained embeddings into the measure of rule quality. RLvRL (Omran, Wang, and Wang 2018) uses quality measures based on embedding similarities to score rules efficiently. The disadvantage of embedding-augmented methods is that training of the embedding model on large KGs itself is not trivial.

1.2 Approach

In this work, we propose the Graph Path Feature Learning (GPFL) system, a novel bottom-up probabilistic inductive rule learner that optimizes rule generation and evaluation using the concept of template rule. A template rule or template is an abstract rule that contains no constants, thus can be used as a template to generate instantiated rules. For example in Figure.1, the rules f_0 and:

$$f_2 = \text{Capital_of}(X, Y) \leftarrow \text{Is_a}(X, Z)$$

are templates, and by replacing variable Z with constant 'Political Center' in f_2 , it is specialized into the instantiated rule p_1 . Inspired by AnyBURL (Meilicke et al. 2019), instead of using a saturation measure that is hard to converge on instantiated rules due to the volume of instantiated rules being extremely large, we propose a novel saturation measure based on templates. Since the size of template space is usually smaller by orders of magnitude than that of the instantiated rules, template saturation is much easier to converge even over all of the allowed lengths, and through our experiments, we show that the size of mined templates has a strong positive correlation with the prediction performance. In particular, GPFL utilizes a two-stage rule generation mechanism which first generalizes ground rules that are randomly sampled from the KG into templates until a pre-defined template saturation is achieved, and then specializes the templates using constants extracted from groundings and positive instances into instantiated rules. Moreover, inspired by the idea of query pack (Blockeel et al. 2002) where structurally similar rules are grouped for collective evaluations, we propose to put instantiated rules derived from the same templates into the same groups, and then evaluate the rules in groups over the groundings of the deriving templates, which substantially decreases the invocations of expensive grounding procedure compared to methods that have to ground every instantiated rule individually.

1.3 Contribution

Our contributions can be summarized as 1.) We propose a novel bottom-up probabilistic inductive rule learner that uses the concept of template for optimized rule generation and evaluation; 2.) To the best of our knowledge, this is the first work that utilizes a two-stage generalization-specialization mechanism to generate rules from KGs; 3.) Through experiments on three large benchmark KGs, we observe that: there exists positive correlation between the size of mined templates and the predictive performance; all of the rule types that are allowed in our language bias contribute to proposing correct top predictions; the performance of GPFL on KGC task consistently and substantially outperforms all of the strong embedding and logic-based baselines over all three popular benchmark datasets.

2 Related Works

In this section, we discuss existing logic-based methods in detail. We give brief introductions to differentiable and reinforcement rule learners and examine inductive rule learners

through the lens of mechanisms employed for rule space exploration.

Neural LP (Yang and Cohen 2017) and DRUM (Sadeghian et al. 2019) are differentiable learners based on the differentiable logic formulation Tensorlog (Cohen 2020) where the traversals over a graph are formulated as sequences of matrix multiplications and logical inferences are compiled into sequences of differentiable operations on matrices. Although the robustness introduced by numerical optimizations is desired, due to the limitations on current architecture designs, existing systems can only learn CARs.

DeepPath (Xiong, Hoang, and Wang 2017), Minerva (Das et al. 2018) and Multi-hop (Lin, Richard, and Caiming 2018) are reinforcement learners that formulate rule generation as a sequential decision-making problem where policy-based agents are trained to find the promising paths potentially connecting positive instances by using rewarding mechanisms based on KG embeddings. Existing works can mine CARs and ground rules, which in many cases is not expressive enough or too specific to describe concepts.

We categorize inductive rule learners based on the mechanisms employed for exploring the target rule space:

- **Specialization-Only (Spec):** Top-down learners such as QuickFOIL (Zeng, Patel, and Page 2014), ScaLeKB (Chen, Wang, and Goldberg 2016) and AMIE+ (Galárraga et al. 2015) generate rules by repeatedly specializing rules derived from a top rule via adding new atoms or instantiating variables in existing atoms. This approach tends to propose groundless rules that invoke the grounding procedure but do not contribute to the inferences. Existing methods use optimized implementation utilizing parallelization and distributed computation for better scalability.
- **Generalization-Only (Gen):** Bottom-up learners such as PRAs (Lao, Minkov, and Cohen 2015), SFE (Gardner and Mitchell 2015), RuleN (Meilicke et al. 2018) and Any-BURL (Meilicke et al. 2019) populate a rule space with rules generalized from paths in KGs. Compared to Spec methods, Gen methods guarantee that there is at least one grounding for generated rules. Since it is impractical to extract all paths on large KGs, strategies prioritizing the extraction of paths inducing valuable rules are utilized. However, existing strategies are often naive or biased to mine short rules.
- **Specialization-Generalization (Spec-Gen):** Classic ILP methods such as Aleph (Srinivasan 2001) and Progol (Muggleton 1995) harness a mechanism that first specializes the top rule into a bottom clause which is a compact representation of a positive instance, and then generate rules by generalizing bottom clauses. As this mechanism is equivalent to apply Gen methods to sub-graphs that contain paths originated from positive instances, it inherits the issues from both Gen and Spec methods to some extend.

In this work, we propose a Generalization-Specialization (Gen-Spec) mechanism that first generalizes paths into templates and then specializes templates into instantiated rules. The saturation of templates as a strategy that controls the

progress of rule generation is used to ease the exploration issue in Gen part, and the grouping technique is used to tackle the inefficiency issue in Spec part.

3 Methodology

A knowledge graph $\mathcal{G} = (\mathcal{E}, \mathcal{R}, \mathcal{T})$ is a directed multi-graph that contains ground atoms in the form of triples $r_i(e_j, e_k) \in \mathcal{T}$ where $r_i \in \mathcal{R}$ is a relation type and $e_j, e_k \in \mathcal{E}$ are entities. In logic term, relation type and entity are called predicate and constant, respectively. A path or ground rule, denoted by:

$$r_0(e_0, e_1), r_1(e_1, e_2), \dots, r_n(e_n, e_{n+1})$$

is a sequence of ground atoms extracted from KGs. The head of a rule is the first atom in a rule, and the rest of atoms are the body atoms. The length of a rule is the count of body atoms. We can rewrite a rule in definite Horn clause form as:

$$r_0(e_0, e_1) \leftarrow r_1(e_1, e_2), \dots, r_n(e_n, e_{n+1})$$

where the head atom $r_0(e_0, e_1)$ is inferred as a prediction for a KG, if all of the body atoms can be grounded in the KG. By replacing constants in ground atoms with variables, we can generalize ground rules into first-order rules for stronger expressiveness.

A KGC query takes the form of $r_t(e_i, ?)$ or $r_t(?, e_i)$ where r_t is the learning target that a rule learner attempts to reason using rules, and the question mark is expected to be replaced with candidates $e \in \mathcal{E}$ suggested by learnt rules such that predictions $r_t(e_i, e)$ or $r_t(e, e_i)$ for target r_t are proposed. Formally, given a knowledge graph \mathcal{G} and a learning target r_t , a discriminative rule learner aims to populate a rule space F with weighted rules $f \in F$ where a rule f has a head atom of type r_t and the weight of f reflects its quality. Once the rule space is populated, weighted rules can then be used for inference by answering KGC queries. The strength of a prediction depends on the quality of rules suggesting it.

3.1 Language Bias

Language bias as a prior knowledge along with semantic bias is used extensively in rule learning methods to restrict rule space by specifying the desired types of rules to include (De Raedt 2008). For bottom-up rule learners that generate rules from paths in KGs, the implicit syntactic restrictions are that only 2-ary atoms are allowed and adjacent atoms are connected by the same variables or constants. We use lower-case letters for constants and upper-case letters for variables where the symbols X and Y denote variables in the head atom, and V_i a variable in the body atoms. In this work, we only consider straight rules where a variable or constant can occur at most twice in the body atoms to avoid cycles. In addition, we do not generate trivial rules that self-loop:

$$r_t(X, Y) \leftarrow r_1(X, V_0), \dots, r_n(V_n, X)$$

or are recursive rules of length 1:

$$r_t(X, Y) \leftarrow r_t(X, Y) \text{ or } r_t(X, e) \leftarrow r_t(X, e)$$

Now we introduce some of the terms used throughout this work. Given a rule:

$$r_t(X, Y) \leftarrow r_1(X, V_0), r_2(V_0, V_1), \dots, r_n(V_n, V_{n+1})$$

we call variable X the original variable in that the body atoms are originated from it; variable Y the free variable; variables such as V_0 the connecting variables in that they connect adjacent atoms, and the non-connecting variable V_{n+1} in the last body atom the tail variable. A rule is closed if the free variable Y is identical to the tail variable V_{n+1} , and is open if the free variable does not occur in the body atoms. A rule is abstract if it contains no constants, otherwise it is instantiated.

In this work, we use following types of rules to make up our language bias:

Template : $r_t(X, Y) \leftarrow r_1(X, V_0), \dots, r_n(V_n, V_{n+1})$
HAR : $r_t(X, e) \leftarrow r_1(X, V_0), \dots, r_n(V_n, V_{n+1})$
BAR : $r_t(X, e_i) \leftarrow r_1(X, V_0), \dots, r_n(V_n, e_j)$
CAR : $r_t(X, Y) \leftarrow r_1(X, V_0), \dots, r_n(V_n, Y)$

a template is an open abstract rule; a head anchored rule (HAR) is a specialization of a template where the free variable is substituted with a constant; a both anchored rule (BAR) is a specialization of a HAR where the tail variable is replaced with a constant, and a CAR, as introduced in previous sections, is a closed abstract rule. Specifically, templates are used as intermediate rules for generating HARs and BARs only, and will not be included in the final rule space for rule application. This is because templates as rules are too general to differentiate predictions. A HAR characterizes potential candidates in relation of r_t to an entity e by a pattern, whereas a BAR highlights a pattern involving the correlation between entities e_i and e_j . A CAR is a base rule type included in language biases employed by most of existing works in that it is often small in size but provides a good base predictive performance.

The reason for selecting these rule types is based on the assumptions of concept stratification and deconstruction. Concept stratification assumes that learning targets have different explanatory complexities, thus rule types of different complexities should be included in the rule space instead of only having rule types of the same complexities. For instance, given a correct prediction $r_t(e_0, e_1)$ and an incorrect one $r_t(e_2, e_1)$, both are suggested by the HAR:

$$r_t(X, e_1) \leftarrow r_1(X, V_0)$$

with confidence α_1 . As they are suggested with the same confidence, the system can not distinguish one from another. This is a case where the rule space is too general for the learning target. When we allow the more specific BAR in the rule space and we know that the BAR:

$$r_t(X, e_1) \leftarrow r_1(X, e_3)$$

predicts $r_t(e_0, e_1)$ with confidence $\alpha_2 \neq \alpha_1$, the system then can treat the predictions differently based on their confidence. The inclusion of both HAR and BAR is an attempt to stratify the concepts that can be expressed by the system for better adaptivity.

Concept deconstruction assumes a complex concept can be expressed by the combination of simple concepts. For instance, a complex rule that has more than one constants in its body atoms is as follow:

$$r_t(X_1, e) \leftarrow r_1(X_1, e_0), r_2(e_0, e_1)$$

Algorithm 1 GPFL Algorithm

Input: $\mathcal{G}, I, sat, bs, tar, len$

Output: F'

```

1: Initialize empty set  $F$ 
2:  $M \leftarrow Generalization(\mathcal{G}, I, sat, bs, len)$ 
3:  $T \leftarrow$  Sort  $M$  by value and select top  $tar$  templates
4: for  $t$  in  $T$  do
5:   if  $t$  is a CAR then
6:      $Score(t)$ 
7:      $F \leftarrow F \cup \{t\}$ 
8:   else
9:      $A \leftarrow Grounding(t, \mathcal{G})$ 
10:     $HARs \leftarrow SpecializeIntoHARs(t, I)$ 
11:     $BARs \leftarrow SpecializeIntoBARs(t, I, A)$ 
12:     $GroupScore(HARs, BARs, A)$ 
13:     $F \leftarrow F \cup HARs \cup BARs$ 
14:   end if
15: end for
16:  $F' \leftarrow Pruner(F)$ 
17: return  $F'$ 

```

and it can be expressed by the conjunction of BARs:

$$r_t(X_2, e) \leftarrow r_1(X_2, e_0) \\ r_t(X_3, e) \leftarrow r_1(X_3, V_0), r_2(V_0, e_1)$$

in that X_1 has the same domain as $X_2 \cap X_3$.

3.2 Algorithm Overview

In this section we introduce the GPFL algorithm and discuss the settings of the learning system. GPFL is a discriminative learner, that is it learns rules for one learning target at a time. Given a target r_t , we denote by I the positive instances of r_t in a KG \mathcal{G} . As shown in Algorithm.1, it utilizes a two-stage Gen-Spec mechanism to populate the rule space. At the first stage, the $Generalization(\mathcal{G}, I, sat, bs, len)$ procedure generalizes the ground rules randomly sampled from neighbourhoods of length len of positive instances into templates and CARs. It also counts the frequency of occurrences of templates in the generalization procedure, and store (template, frequency) pairs in the frequency map M . For simplicity, we also save (CAR, frequency) pairs in M . We observe that targets in large KGs usually have many templates but only a portion of the templates are frequent patterns shared by positive instances. Therefore, GPFL sorts map M by frequency in descending order, and select CARs and top tar templates for specialization.

Once the algorithm has produced the CARs and a selection of top templates, it proceeds to the second stage - specialization. We define a scoring function $Score(f)$ that measures quality of rules. The standard confidence (Galárraga et al. 2015), a popular quality measure, for a given rule f is defined as:

$$sc(f) = \frac{Supp}{Ground} \quad (1)$$

where support $supp$ is the correct predictions that f makes over \mathcal{G} , and $Ground$ is the total predictions suggested by

f. We use a smoothed confidence measure (Meilicke et al. 2019) that mitigates the bias to rules that make a few predictions but have higher confidence than ones making a lot predictions by adding an user-defined offset η to the denominator as:

$$ssc(f) = \frac{Supp}{\eta + Ground} \quad (2)$$

As stated in Algorithm.1 from line 4, for each CAR, GPFL simply scores it and put it in the rule space F . For each template t , the $Grounding(t, \mathcal{G})$ procedure generates groundings A based on t . A template is then specialized into HARs and BARs using constants occurred in instances I and groundings A . The generated HARs and BARs are evaluated collectively in the function $GroupScore(HARs, BARs, A)$ using groundings of the deriving template t , and then added to the rule space F . A $Pruner(F)$ function is employed to prune rules having quality measures below user-defined support and confidence threshold. Eventually, GPFL returns a rule space composed of quality CARs, HARs and BARs that have head atoms of type r_t and lengths within the user-defined range len .

3.3 Rule Generation

GPFL generates rules using both generalization and specialization. Algorithm.2 shows the generalization procedure. The system first samples an instance i from I , and applies $PathSampler(\mathcal{G}, i, len)$ which uses random walkers to traverse the neighbourhood of i to sample paths P . For each path $p \in P$, GPFL generalizes it into a template t by replacing all constants in p with variables. A newly generated template t is first put into the current batch T , and then used to update the frequency map M , that is if t exists in M , its frequency increments by 1, otherwise a new entry $(t, 1)$ is put into M . A user-defined batch size bs is used to control the interval between saturation checks. When the path count $count$ is a multiple of bs , current saturation sat' is updated by computing the proportion of known templates in current batch, and if sat' is greater than sat , the procedure will terminate and return the frequency map, otherwise a new iteration will start to generate more templates until the template saturation is achieved.

In the specialization procedure (lines 9-13 in Algorithm.1), procedure $SpecializeIntoHARs(t, I)$ substitutes the free variable of template t with distinct constants at the corresponding position in positive instances I . For instance, assume we have a template:

$$t_0 = r_t(X, Y) \leftarrow r_1(Y, V_0)$$

where X is the free variable and Y the original variable, and positive instances:

$$I_0 = \{r_t(e_0, e_1), r_t(e_0, e_2), r_t(e_1, e_3)\}$$

the substitutions for the free variable thus are $\{e_0, e_1\}$. A possible HAR that can be created from this example is:

$$o_0 = r_t(e_0, Y) \leftarrow r_1(Y, V_0)$$

Procedure $SpecializeIntoBARs(t, I, A)$ substitutes the free and tail variables simultaneously with distinct pairs of

Algorithm 2 Generalization

Input: $\mathcal{G}, I, sat, bs, len$

Output: M

```

1: Initialize empty set  $T$  and empty map  $M$ 
2:  $count \leftarrow 0$ 
3: do
4:    $i \leftarrow$  Randomly sample an instance from  $I$ 
5:    $P \leftarrow PathSampler(\mathcal{G}, i, len)$ 
6:   for  $p$  in  $P$  do
7:      $count \leftarrow count + 1$ 
8:      $t \leftarrow CreateTemplates(p)$ 
9:      $T \leftarrow T \cup t$ 
10:    Update  $M$  with  $t$ 
11:    if  $mod(count, bs) == 0$  then
12:       $sat' \leftarrow \frac{|M.keys \cap T|}{|T|}$ 
13:       $T \leftarrow \emptyset$ 
14:    end if
15:   end for
16: while  $sat' < sat$ 
17: return  $M$ 

```

constants that are at the corresponding positions in instances I and groundings A respectively, and are joined by the constants at the position of original variable. For instance, assume we have template t_1 and positive instances I_0 , now also have groundings of the template:

$$A_0 = \{r_1(e_1, e_2), r_1(e_2, e_3), r_1(e_3, e_4)\}$$

we can create a substitution pair (e_0, e_2) because instance $r_t(e_0, e_1)$ and grounding $r_1(e_1, e_2)$ are joined by constant e_1 such that e_0 takes the place of the free variable and e_1 takes that of the tail variable. A BAR generated with this pair is:

$$o_1 = r_t(e_0, Y) \leftarrow r_1(Y, e_2)$$

other pairs that can be inferred from this example are (e_0, e_3) and (e_1, e_4) . This specialization mechanism shares the same issue of grounding groundless rules for evaluation with existing Spec works in that the instantiated rules are created by templates and constants instead of being generalized directly from ground rules. We propose an optimized rule evaluation mechanism to mitigate the overheads introduced by this issue.

3.4 Collective Rule Evaluation

It is obvious that the instantiated rules derived from the same templates share the same sequence of composing predicates. This structural similarity introduced by deductive dependencies between rules motivates us to put instantiated rules derived from the same templates into the same groups for collective evaluation over the groundings of the deriving templates. We denote by O_t the group containing rules specialized from the template t . For instance, given template t_0 , HAR o_0 and BAR o_1 from previous example, we can infer $o_0, o_1 \in O_{t_0}$. Assume t_0 only has groundings A_0 , to evaluate the quality of o_0 and o_1 , most of the existing works need to ground o_0 and o_1 individually, which ignores the fact that

Data	#Entities	#Types	#Triples	Degree
FB15K-237	14541	237	310116	21.32
WN18RR	40943	11	93003	2.27
NELL-995	75492	200	154213	2.04

Table 1: Statistics of the benchmark datasets.

the groundings of o_0 and o_1 are merely different subsets of A_0 . Therefore, by only invoking the expensive grounding procedure once on template t_0 to produce A_0 , we can evaluate both o_0 and o_1 using A_0 instead of querying groundings for o_0 and o_1 using two separate grounding invocations. In this way, we can substantially reduce the number of invocations of expensive grounding procedure to avoid a significant number of redundant computations on large KGs.

3.5 Rule Application

With rules proposed in Algorithm.1, GPFL is ready to answer queries about the learning target r_t . When operating on large KGs, the quantity of instantiated rules can be easily over tens of millions, which often causes scalability issue in rule application, especially for in-memory implementations. To balance the scalability and model quality, GPFL sorts the instantiated rules in each group by confidence in descending order, and only applies the top tir instantiated rules in each group along with CARs to make predictions. For instance, if we have 1000 templates, 500 CARs and tir set to 10, then there are at most $1000 \times 10 + 500 = 10500$ rules in total for rule application.

The rules are grounded over the KG with testing instances removed to avoid the possibility of any kind of trivial rules making predictions using testing instances. The groundings are then treated as predictions to answer KGC queries. As a prediction can be suggested by multiple rules, it introduces complexity in ranking the predictions. In this work, we use the maximum aggregation strategy proposed in AnyBURL (Meilicke et al. 2019) to rank predictions. In particular, predictions are sorted by the maximum of the confidence of rules suggesting the predictions, and if there are ties among predictions, the tied predictions are sorted by recursively comparing the next highest confidence of suggesting rules until all ties are resolved.

4 Experiments

In this section, we examine the GPFL system through experiments over three large benchmark KGs. Specifically, we report correlation analyses between system parameters and predictive performance, performance results on KGC task in comparison to baselines, and an analysis on composition of rules contributing to make top correct predictions.

4.1 Experiments Setup

Datasets We select the FB15K-237 (Toutanova and Chen 2015), WN18RR (Dettmers et al. 2018) and NELL-995 (Xiong, Hoang, and Wang 2017) datasets for evaluation. FB15K-237 and WN18RR are modified version of the original datasets proposed in (Bordes et al. 2013) to avoid testing

set leakage introduced by inverse relations of testing set being present in the training set. In particular, WN18RR only removes the redundant inverse relations, whereas FB15K-237 removes both redundant inverse relations and factual mutual relations of the same type, which makes it a less realistic benchmark. The NELL-995 complements FB15K-237 and WN18RR in that it has more relation types than WN18RR and smaller degree than FB15K-237, which allows it to have medium-sized yet diverse rule space. Table.1 shows the statistics of the benchmarks.

Implementation GPFL is implemented in Java on top of the core Neo4j API¹. All experiments are performed on AWS EC2 instances that have 8 CPU cores and 64GB RAM. GPFL allows flexible control on scalability by adjusting hyper-parameters to accommodate the specification of running machines. For scalability-related parameters, we set them to values that push running machines to limit. We set performance-related parameters as follows: length len to 3, template sample size tar to 500, instantiated rule sample size tir to 500, saturation sat to 0.999, batch size bs to 100000, support threshold to 1 and confidence threshold to 0.0001. The source code of GPFL and datasets used in the paper have been made available at <https://github.com/irokin/GPFL>.

Evaluation Protocol We follow the evaluation protocol proposed in (Bordes et al. 2013) and (Omran, Wang, and Wang 2018) to adapt inductive rule learners to KGC task. GPFL answers both head queries $r_t(?, e)$ and tail queries $r_t(e, ?)$ that are created by corrupting testing instances. For measuring the predictive performance, we report hits@1, hits@3, hits@10 and mean reciprocal rank (MRR), all in the filtered setting.

4.2 Correlation Analysis

In this section, we perform a sensitivity analysis on the impact of batch size bs and template saturation sat to the size of mined templates, and more importantly, we examine if the size of mined templates is positively correlated to the predictive performance to justify the use of template saturation to control the progress of rule generation.

As illustrated in Figure.2, we randomly select 4 targets from FB15K-237 and NELL-995 for analysis, respectively. The heatmaps demonstrate the difference in template size when different (bs, sat) configurations are employed. The color of each cell reflects the size of mined templates. For each cell, we run the system 5 times with the same training and testing sets, and report the average template size. By randomly picking a cell, and comparing the increase in template size between moving one cell right and up, we observe that sat and bs have similar and individually small impact on the size of mined templates. Therefore, one needs to tune up both sat and bs to obtain more templates.

The template size vs MRR diagrams in Figure.2 demonstrate the correlation between MRR and the size of mined templates. Each of the diagram is created over the smoothed experiment results used to create the heatmaps. Specifically,

¹<https://github.com/neo4j/neo4j>

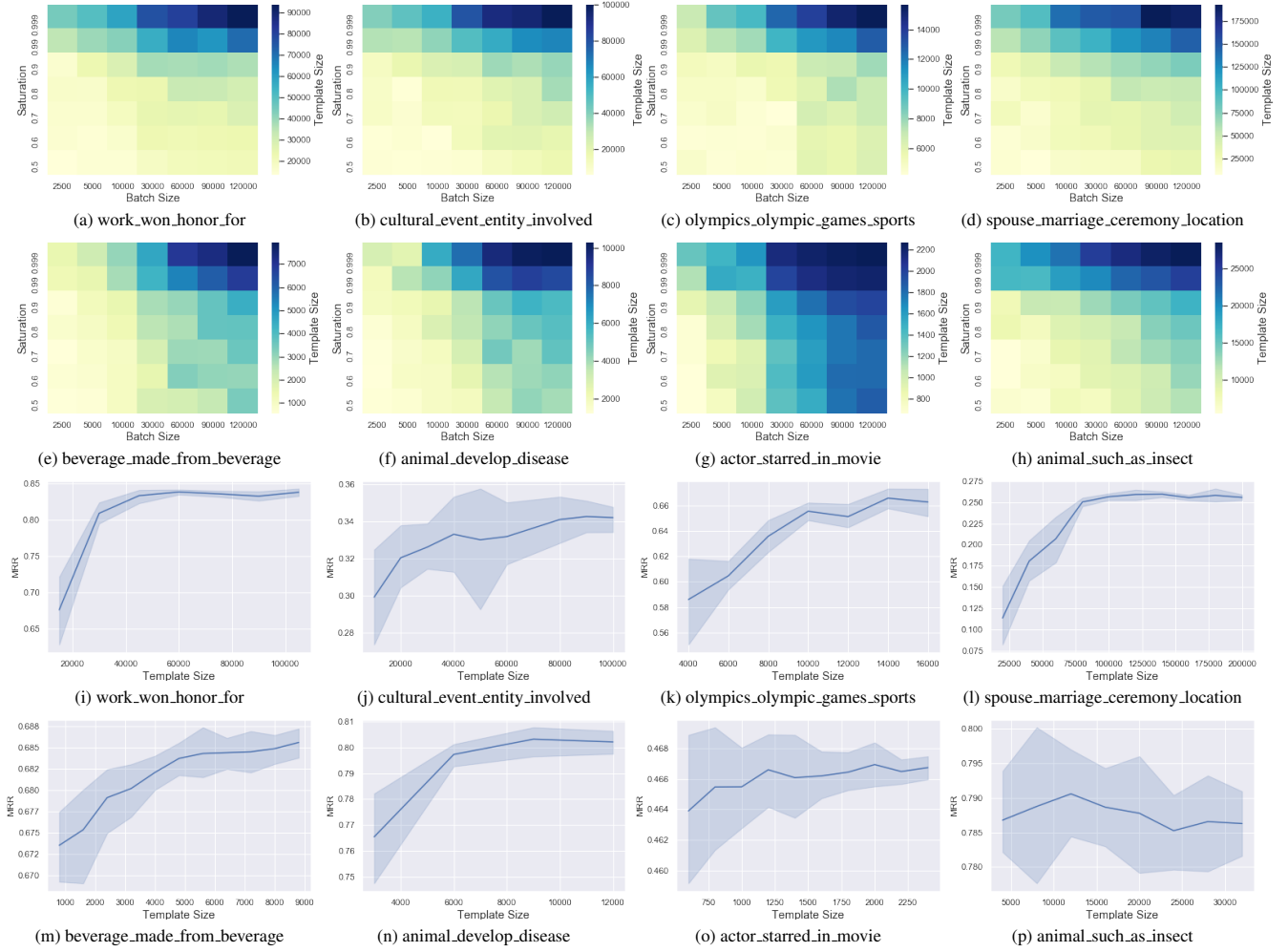


Figure 2: Heatmaps and template size vs MRR diagrams for correlation analysis. The sub-captions are the names of targets in the datasets. Diagrams (a)-(d) and (i)-(l) are heatmaps and template size vs MRR diagrams, respectively, for targets selected from FB15K-237, and (e)-(h) and (m)-(p) are for targets from NELL-995.

as each heatmap has 49 cells, with each cell value obtained from 5 experiment results, we have in total 245 (template size, MRR) data points for drawing a MRR vs template diagram. Based on the range of template sizes for different targets, we smooth the line by grouping data points that fall into the same range, e.g., [1000, 1500] or [2000, 4000], into a new aggregated data point, and report its mean and standard deviation. For instance, Figure.2i shows that there is a dramatic increase in performance between size 20000 to 40000, and then it flattens due to all expressive templates are extracted. Figure.2p shows a different scenario where the MRR fluctuates in a small range with increasing template size. This is because the expressive templates are already extracted within the size of 5000. Overall, we observe that there exists a strong positive correlation between the template size and the predictive performance, which justifies our choice of template saturation for controlling the progress of rule generation.

4.3 Knowledge Graph Completion

In this section, we evaluate the effectiveness of GPFL on KGC task in comparison to state-of-the-art baselines. Through experiments, we show that GPFL, a classic inductive rule learner, is the best performing model on KGC task over embedding and other logic-based models, and wins by large margin.

Table.2 is a comparison table that includes the experiment results of 11 embedding models and 5 logic-based models on FB15K-237 and WN18RR datasets. The DistMult (Yang et al. 2015) result is taken from CompGCN (Vashishth et al. 2020b) paper; the Neural LP (Yang and Cohen 2017) result is obtained from the DRUM (Sadeghian et al. 2019) paper, and the AMIE+ (Galárraga et al. 2015) and RuleN (Meilicke et al. 2018) results are taken from the AnyBURL (Meilicke et al. 2019) paper. All other results are taken directly from the corresponding papers. Table.3 shows the experiment results on NELL-995 dataset where 5 embedding models and the AnyBURL are compared with GPFL. The

	FB15K-237				WN18RR			
	MRR	Hits@10	Hits@3	Hits@1	MRR	Hits@10	Hits@3	Hits@1
DistMult (Yang et al. 2015)	.241	.419	.263	.155	.430	.490	.440	.390
ComplEx (Trouillon et al. 2016)	.247	.428	.275	.158	.440	.510	.460	410
ConvE (Dettmers et al. 2018)	.316	.491	.350	.239	.460	.480	.430	.390
R-GCN+ (Schlichtkrull et al. 2018)	.249	.417	.264	.151	-	-	-	-
TuckER (Balazevic, Allen, and Hospedales 2019)	.358	.544	.394	.266	.470	.526	.482	.443
RotatE (Sun et al. 2019)	.338	.533	.375	.241	.476	.571	.492	.428
SACN (Shang et al. 2019)	.360	.550	.400	.270	.470	.540	.480	.430
QuatE (Zhang et al. 2019)	.366	.556	.401	.271	.488	.582	.508	.438
InteractE (Vashisht et al. 2020a)	.354	.535	-	.263	.463	.528	-	.430
HAKE (Zhang et al. 2020)	.346	.542	.381	.250	.497	.582	.516	.452
CompGCN (Vashisht et al. 2020b)	.355	.535	.390	.264	.469	.546	.494	.443
AMIE+ (Galárraga et al. 2015)	-	.409	-	.174	-	.388	-	.358
Neural LP (Yang and Cohen 2017)	.240	.362	-	-	.435	.566	.434	.371
RuleN (Meilicke et al. 2018)	-	.420	-	.182	-	.536	-	.427
DRUM (Sadeghian et al. 2019)	.343	.516	.378	.255	.486	.586	.513	.425
AnyBURL (Meilicke et al. 2019)	.310	.486	-	.233	.470	.552	-	.446
GPFL (proposed method)	.549	.631	.535	.477	.570	.654	.627	.600
	±.048	±.045	±.045	±.047	±.010	±.009	±.010	±.012

Table 2: KGC experiment results on FB15K-237 and WN18RR. The top section contains embedding models; the middle section includes the logic-based methods; and the bottom section states the GPFL results and standard deviations. Best results in each section are highlighted with underscore, and the best results over all models are indicated in bold.

NELL-995				
	MRR	Hits@10	Hits@3	Hits@1
DistMult (Yang et al. 2015)	.485	.610	.524	.401
ComplEx (Trouillon et al. 2016)	.482	.606	.528	.399
ConvE (Dettmers et al. 2018)	.491	.613	.531	.403
R-GCN+ (Schlichtkrull et al. 2018)	.120	.188	.126	.082
KBAT (Nathani et al. 2019)	.530	.695	.564	.447
AnyBURL (our results)	.317	.434	.346	.256
GPFL (proposed method)	.595	.713	.634	.562
	±.042	±.048	±.043	±.045

Table 3: KGC experiment results on NELL-995. The top sections contains competing models where the best results are highlighted with underscore, and the bottom section contains GPFL results and standard deviations. The best results over all models are indicated in bold.

DistMult, ComplEx (Trouillon et al. 2016) and R-GCN+ (Schlichtkrull et al. 2018) results are taken from the KBAT (Nathani et al. 2019) paper, and the AnyBURL result is obtained from our implementation with saturation set to 0.99, length to 3 (both cyclic and acyclic), running time to 1000s and all other settings to default.

For FB15K-237 and NELL-995 datasets, we randomly select 20 targets from all of the relation types in the KG in each run, which means the batch of selected targets are very likely to be different between runs. This is one of the main reason why GPFL results have large deviation on FB15K-237 and NELL-995. For the WN18RR dataset, the system learns rules for all of the 11 types in it. In each run, the positive instances of selected targets are split into training and testing sets in a 7 to 3 ratio. This is different from some of the other models that are evaluated using the same training and testing sets over all runs, and it is another source of deviation. During the rule learning process, triples in testing sets are removed from the KG such that testing sets have no impact on

the rules learnt using training sets. For each dataset, we perform 10 runs and report the average performance. Therefore, each metric of GPFL reported on FB15K-237 and NELL-995 is the mean of 200 trials (20 targets \times 10 runs), and on WN18RR, it is the mean of 110 trials (11 targets \times 10 runs).

We observe substantial and consistent performance improvements over all three benchmarks compared to strong baselines. Especially on FB15K-237, GPFL outperforms the best performing model QuatE (Zhang et al. 2019) by 50% in MRR, and has an average 41% performance gain over hits@n. On WN18RR, the average performance gain of GPFL over the best performing model HAKE (Zhang et al. 2020) is 22% over hits@n, and 13% in MRR. Finally on NELL-995, GPFL has a 24% average performance gain compared to the best model KBAT (Nathani et al. 2019) over hits@n, and 27% in MRR.

4.4 Rule Composition Analysis

To understand what contributes to the improvements on predictive performance, we analyse the composition of rules that suggest top correct predictions. For each KGC run, we record the correct answers in the top 20 answers to queries of the target, and store the rules suggesting these correct predictions in a verification set. We visualize the proportion of rules of different types in the verification sets in Figure.3 where the bar charts at each row show the rule compositions of 3 randomly selected targets and the aggregation of a collection of targets in a dataset. The y-axis indicates the percentage a type of rule takes and the x-axis indicates different rule length.

In Figure.3, the first row shows results from FB15K-237. Figure.3a shows that the CARs of length 3 contribute the most to the correct predictions of ‘film_executive_produced_by’ target while the rules of

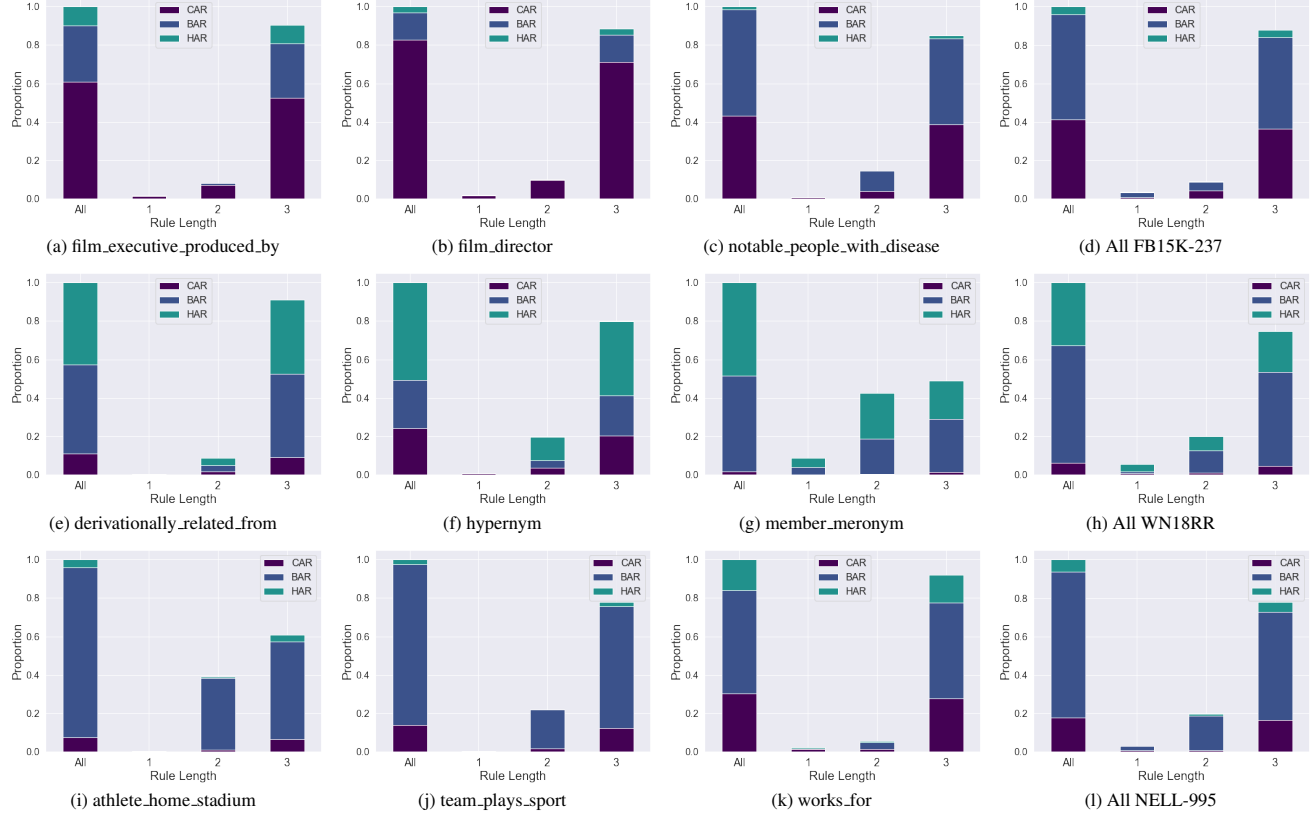


Figure 3: Diagrams for rule composition analysis. Each diagram demonstrates the proportions of rules of different lengths in the rule space that contains top rules suggesting correct predictions. Diagrams (a)-(d) are for targets from FB15K-237; (e)-(h) for targets from WN18RR, and (i)-(l) for targets from NELL995.

length 1 make up near zero contribution, which reflects the removal of inverse redundancies in FB15K-237. Figure.3d shows the aggregated composition over 20 randomly selected targets in FB15K-237. Overall on FB15K-237, we observe that the rules of length 3 contribute the most, and both CARs and BARs are important contributors to making correct predictions. The second row demonstrates results of the WN18RR dataset. In comparison to FB15K-237 results, the HARs take more important roles whereas the CARs are not as important. Figure.3f shows a relatively balanced distribution of all 3 types of rules, which suggests different types of rules are complementing each other to better express the target. Figure.3h shows the aggregated composition over all 11 targets in the dataset. The third row shows the results of NELL-995 dataset where BARs take the dominance. Figure.3l shows the aggregated composition of 20 randomly selected targets in the dataset. Based on the observations, we argue the performance improvements of GPFL over other models are mainly attributed to the choice of language bias which includes conceptually stratified types of rules and the capability of efficiently generating quality instantiated rules of all allowed lengths.

5 Conclusion

In this paper, we present the GPFL system, a bottom-up probabilistic inductive rule leaner that efficiently mines first-order rules for inductive and interpretable inference. We optimize the rule generation and evaluation procedure by using the concept of template rule. Through extensive experiments on large benchmark datasets, experiment results suggest that GPFL outperforms state-of-the-art models by large margin over all testing datasets. We demonstrate the positive correlation between the size of mined templates and the predictive performance. Moreover, by analysing the composition of rules suggesting the top correct predictions, the observations suggest that all three types of rules included in our language bias contribute to making the correct predictions, and the rules of length 3 are the main contributors.

It is interesting that the ubiquitously available deductive dependencies between rules can be utilized for optimizing bottom-up rule learners by incorporating simple saturation and grouping strategy. Although the rule hierarchy is used extensively in top-down learners for exploring rule space, we argue as a direction for future work that there is a potential of exploiting well-structured rule hierarchy that contains both inductive and deductive dependencies between rules to further optimize rule learners.

References

Balazevic, I.; Allen, C.; and Hospedales, T. 2019. TuckER: Tensor Factorization for Knowledge Graph Completion. In *EMNLP*, 5184–5193.

Blockeel, H.; Dehaspe, L.; Demoen, B.; Janssens, G.; Ramon, J.; and Vandecasteele, H. 2002. Improving the efficiency of inductive logic programming through the use of query packs. *JAIR* 16:135–166.

Bollacker, K.; Evans, C.; Paritosh, P.; Sturge, T.; and Taylor, J. 2008. Freebase: a collaboratively created graph database for structuring human knowledge. In *SIGMOD*, 1247–1250.

Bordes, A.; Usunier, N.; Weston, J.; and Yakhnenko, O. 2013. Translating Embeddings for Modeling Multi-Relational Data. In *NIPS*, 2787–2795.

Cai, H.; Zheng, V. W.; and Chang, K. C.-c. 2018. A Comprehensive Survey of Graph Embedding : Problems , Techniques and Applications. *TKDE* 30(9):1616–1637.

Chen, Y.; Wang, D. Z.; and Goldberg, S. 2016. ScaLeKB: scalable learning and inference over large knowledge bases. *VLDB Journal* 25(6):893–918.

Cohen, W. W. 2020. TensorLog : A Probabilistic Database Implemented Using Deep-Learning Infrastructure. *JAIR* 67:285–325.

Das, R.; Dhuliawala, S.; Zaheer, M.; Vilnis, L.; Durugkar, I.; Krishnamurthy, A.; Smola, A.; and Mccallum, A. 2018. Go for a walk and arrive at the answer: Reasoning over paths in knowledge bases using reinforcement learning. In *ICLR*.

De Raedt, L. 2008. *Logical and relational learning*. Springer Science & Business Media.

Dettmers, T.; Minervini, P.; Stenetorp, P.; and Riedel, S. 2018. Convolutional 2D Knowledge Graph Embeddings. In *AAAI*, 1811–1818.

Galárraga, L.; Teflioudi, C.; Hose, K.; and Suchanek, F. M. 2015. Fast rule mining in ontological knowledge bases with AMIE+. *VLDB Journal* 24(6):707–730.

Gardner, M., and Mitchell, T. 2015. Efficient and Expressive Knowledge Base Completion Using Subgraph Feature Extraction. In *EMNLP*, 1488–1498.

Guo, S.; Wang, Q.; Wang, L.; Wang, B.; and Guo, L. 2018. Knowledge Graph Embedding with Iterative Guidance from Soft Rules. In *AAAI*, 4816–4823.

Ho, V. T.; Stepanova, D.; Gad-Elrab, M. H.; Kharlamov, E.; and Weikum, G. 2018. Rule learning from knowledge graphs guided by embedding models. In *ISWC*, 72–90.

Hoffart, J.; Suchanek, F. M.; Berberich, K.; and Weikum, G. 2013. YAGO2: A spatially and temporally enhanced knowledge base from Wikipedia. *Artificial Intelligence* 194:28–61.

Lao, N.; Minkov, E.; and Cohen, W. 2015. Learning Relational Features with Backward Random Walks. In *ACL*, 666–675.

Lao, N.; Mitchell, T.; and Cohen, W. W. 2011. Random Walk Inference and Learning in A Large Scale Knowledge Base. In *EMNLP*, 529–539.

Lin, X. V.; Richard, S.; and Caiming, X. 2018. Multi-Hop Knowledge Graph Reasoning with Reward Shaping. In *ACL*, 3243–3253.

Meilicke, C.; Fink, M.; Wang, Y.; Ruffinelli, D.; Gemulla, R.; and Stuckenschmidt, H. 2018. Fine-grained evaluation of rule- and embedding-based systems for knowledge graph completion. In *ISWC*, 3–20.

Meilicke, C.; Chekol, M. W.; Ruffinelli, D.; and Stuckenschmidt, H. 2019. Anytime Bottom-Up Rule Learning for Knowledge Graph Completion. In *IJCAI*, 3137–3143.

Mitchell, T.; Cohen, W.; Hruschka, E.; Talukdar, P.; Yang, B.; Betteridge, J.; Carlson, A.; Dalvi, B.; Gardner, M.; Kisiel, B.; Krishnamurthy, J.; Lao, N.; Mazaitis, K.; Mohamed, T.; Nakashole, N.; Platanios, E.; Ritter, A.; Samadi, M.; Settles, B.; Wang, R.; Wijaya, D.; Gupta, A.; Chen, X.; Saparov, A.; Greaves, M.; and Welling, J. 2018. Never-ending learning. *Communications of the ACM* 61(5):103–115.

Muggleton, S. 1995. Inverse entailment and progl. *New Generation Computing* 13(3-4):245–286.

Nathani, D.; Chauhan, J.; Sharma, C.; and Kaul, M. 2019. Learning Attention-based Embeddings for Relation Prediction in Knowledge Graphs. In *ACL*.

Niu, G.; Zhang, Y.; Li, B.; Cui, P.; Liu, S.; Li, J.; and Zhang, X. 2020. Rule-Guided Compositional Representation Learning on Knowledge Graphs. In *AAAI*.

Omran, P. G.; Wang, K.; and Wang, Z. 2018. Scalable rule learning via learning representation. In *IJCAI*, 2149–2155.

Pellissier, T.; Stepanova, D.; Razniewski, S.; Mirza, P.; and Weikum, G. 2017. Completeness-aware Rule Learning from Knowledge Graphs. In *ISWC*.

Sadeghian, A.; Armandpour, M.; Ding, P.; and Wang, D. Z. 2019. DRUM: End-To-End Differentiable Rule Mining On Knowledge Graphs. In *NIPS*, 1–13.

Schlichtkrull, M.; B, T. N. K.; Bloem, P.; Berg, R. V. D.; Titov, I.; and Welling, M. 2018. Modeling Relational Data with Graph Convolutional Networks. In *ESWC*, volume 10843, 593–607. Springer International Publishing.

Shang, C.; Tang, Y.; Huang, J.; Bi, J.; He, X.; and Zhou, B. 2019. End-to-end Structure-Aware Convolutional Networks for Knowledge Base Completion. In *AAAI*.

Srinivasan, A. 2001. The aleph manual.

Sun, Z.; Deng, Z.-h.; Nie, J.-y.; and Tang, J. 2019. Rotate: Knowledge graph embedding by relational rotation in complex space. In *ICLR*, 1–18.

Toutanova, K., and Chen, D. 2015. Observed versus latent features for knowledge base and text inference. In *Proceedings of the 3rd Workshop on Continuous Vector Space Models and their Compositionality*, 57–66.

Trouillon, T.; Welbl, J.; Riedel, S.; Gaussier, E.; and Bouchard, G. 2016. Complex Embeddings for Simple Link Prediction. In *ICML*, volume 48.

Vashisht, S.; Sanyal, S.; Nitin, V.; Agrawal, N.; and Talukdar, P. 2020a. InteractE: Improving Convolution-based

Knowledge Graph Embeddings by Increasing Feature Interactions. In *AAAI*.

Vashishth, S.; Sanyal, S.; Nitin, Vikram; and Talukdar, P. 2020b. Composition-based multi-relational graph convolutional networks. In *ICLR*, 1–15.

Xiong, W.; Hoang, T.; and Wang, W. Y. 2017. DeepPath : A Reinforcement Learning Method for Knowledge Graph Reasoning. In *ACL*, 564–573.

Yang, F., and Cohen, W. W. 2017. Differentiable Learning of Logical Rules for Knowledge Base Reasoning. In *NIPS*.

Yang, B.; Yih, W.-t.; He, X.; Gao, J.; and Deng, L. 2015. Embedding entities and relations for learning and inference in knowledge bases. In *ICLR*, 1–13.

Zeng, Q.; Patel, J.; and Page, D. 2014. QuickFOIL: Scalable Inductive Logic Programming. *VLDB* 8(3):197–208.

Zhang, S.; Tay, Y.; Yao, L.; and Liu, Q. 2019. Quaternion Knowledge Graph Embeddings. In *NeurIPS*, number 1, 1073–1080.

Zhang, Z.; Cai, J.; Zhang, Y.; and Wang, J. 2020. Learning Hierarchy-Aware Knowledge Graph Embeddings for Link Prediction. In *AAAI*.

Zhou, J.; Cui, G.; Zhang, Z.; Yang, C.; Liu, Z.; and Sun, M. 2019. Graph Neural Networks: A Review of Methods and Applications. In *Arxiv*, 1–20.